4278 *Inorg. Chem.* **2010**, *49*, 4278–4287
DOI: 10.1021/ic100145e

Inorganic Chemistry
Article

2-Anthryltriazolyl-Containing Multidentate Ligands: Zinc-Coordination Mediated Photophysical Processes and Potential in Live-Cell Imaging Applications

Heather A. Michaels,[†] Christopher S. Murphy,[‡] Ronald J. Clark,[†] Michael W. Davidson,*[,‡] and Lei Zhu*[,†]

[†]*Department of Chemistry and Biochemistry, Florida State University, Tallahassee, Florida 32306-4390, and* [‡]*National High Magnetic Field Laboratory and Department of Biological Science, Florida State University, 1800 East Paul Dirac Drive, Tallahassee, Florida 32310*

Received January 23, 2010

1,2,3-Triazol-4-yl (triazolyl)-containing tetradentate ligand **1** undergoes fluorescence enhancement upon binding to zinc ion (Zn^{2+}) in both organic (acetonitrile) and aqueous solutions. A 1:1 complex of **1** with a trigonal bipyramidal Zn^{2+} was characterized by X-ray crystallography. The cyclic voltammogram (CV) of **1** suggests that an intramolecular photoinduced electron transfer (PET) process is thermodynamically feasible which would quench the fluorescence of the 2-anthryltriazolyl fluorophore. On the basis of the X-ray and CV data, it was initially postulated that the 1:1 binding between Zn^{2+} and ligand **1** shuts down the PET quenching pathway of the free ligand, which leads to the fluorescence enhancement of **1**. However, the nuance of the interaction between **1** and Zn^{2+} was revealed by isothermal titration calorimetry (ITC) and ^{1}H NMR titration experiments. A two-step binding process was observed which proceeds through an intermediate species of 2:1 (ligand/Zn^{2+}) stoichiometry. Upon close examination of the fluorescence spectra of **1** during the Zn^{2+} titration experiment, the fluorescence profile is in fact consistent with a two-step binding process in which a moderate fluorescence enhancement was observed during the early stage of the titration, followed by a bathochromic shift in conjunction with a more pronounced enhancement as Zn^{2+} concentration increases. The studies on compounds **2**−**5** support the amended hypothesis that upon increasing Zn^{2+} concentration, compound **1** first undergoes fluorescence enhancement because of the formation of a 2:1 (ligand to Zn^{2+}) complex which slows down the PET quenching process. As Zn^{2+} concentration increases, the 2:1 complex is converted into a 1:1 complex which facilitates an intramolecular exciplex formation between the excited 2-anthryltriazolyl fluorophore and the Zn^{2+}-bound pyridyl moiety. Finally, the potential of compound **1** as an intracellular fluorescent indicator for Zn^{2+} was evaluated. HeLa cells loaded with compound **1** grown in Zn^{2+}-rich media show stronger fluorescence than those grown under Zn^{2+}-deprived conditions, confirming the promise that the triazolyl-containing polyaza fluoroionophores can be developed into intracellular fluorescent indicators targeting biological Zn^{2+}.

Introduction

The Cu(I)-catalyzed Huisgen cycloaddition between a terminal alkyne and a carbon azide (CuAAC) was developed by the groups of Sharpless and Meldal in 2002.[1−3] This reaction (a) affords a single regioisomer of 1,4-substituted 1,2,3-triazoles, (b) is rapid under almost any conditions, and (c) demonstrates the exclusive reactivity between the terminal alkyne and the carbon azide in the presence of Cu(I).[3] These unique advantages have propelled the CuAAC reaction to become one of the most widely employed organic reactions in the past decade in areas including drug discovery,[4] bioconjugation,[5] and materials science.[6] In most cases, the triazole ring resulting from the coupling reaction has served as a passive linker for joining the rich functionalities carried by the alkyne and azide components. On the functional side, the 1,2,3-triazolyl group has been recognized to possess a large dipole moment (> 5 D),[7,8] to participate in hydrogen bonding,[9,10] and to bind biomolecules through various noncovalent interactions.[11] Recently, the ability of 1,2,3-triazoles to

*To whom correspondence should be addressed. E-mail: lzhu@chem.fsu.edu (L.Z.), davidson@magnet.fsu.edu (M.W.D.).

(1) Rostovtsev, V. V.; Green, L. G.; Fokin, V. V.; Sharpless, K. B. *Angew. Chem., Int. Ed.* **2002**, *41*, 2596–2599.
(2) Tornøe, C. W.; Christensen, C.; Meldal, M. *J. Org. Chem.* **2002**, *67*, 3057–3064.
(3) Meldal, M.; Tornøe, C. W. *Chem. Rev.* **2008**, *108*, 2952–3015.
(4) Kolb, H. C.; Sharpless, K. B. *Drug Discovery Today* **2003**, *8*, 1128–1137.
(5) Prescher, J. A.; Bertozzi, C. R. *Nat. Chem. Biol.* **2005**, *1*, 13–21.
(6) Lutz, J.-F. *Angew. Chem., Int. Ed.* **2007**, *46*, 1018–1025.
(7) Bourne, Y.; Kolb, H. C.; Radic, Z.; Sharpless, K. B.; Taylor, P.; Marchot, P. *Proc. Natl. Acad. Sci. U.S.A.* **2004**, *101*, 1449–1454.
(8) Angelo, N. G.; Arora, P. S. *J. Am. Chem. Soc.* **2005**, *127*, 17134–17135.
(9) Horne, W. S.; Yadav, M. K.; Stout, C. D.; Ghadiri, M. R. *J. Am. Chem. Soc.* **2004**, *126*, 15366–15367.
(10) Brik, A.; Alexandratos, J.; Lin, Y.-C.; Elder, J. H.; Olson, A. J.; Wlodawer, A.; Goodsell, D. S.; Wong, C.-H. *ChemBioChem* **2005**, *6*, 1167–1169.
(11) Srinvasachari, S.; Liu, Y.; Zhang, G.; Prevette, L.; Reineke, T. M. *J. Am. Chem. Soc.* **2006**, *128*, 8176–8184.

 Published on Web 04/06/2010

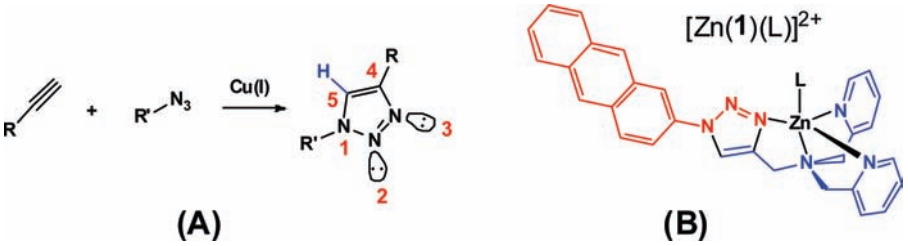

Figure 1. (A) Cu(I)-catalyzed azide−alkyne cycloaddition (CuAAC) to afford a 1,4-substituted 1,2,3-triazole; (B) the Zn^{2+} complex of the fluorescent tetradentate ligand **1**. Red: the azide component; Blue: the alkyne component; L: a coordinating solvent molecule; e.g., acetonitrile.

coordinate metal ions has been explored in a number of studies.[12] Notably, triazolyl-containing compounds have been developed as fluorescent indicators for metal ions,[13−16] delivery systems for metal-based therapeutic agents and radioactive labels,[17−21] accelerating ligands in organometallic catalysis,[22−27] and supramolecular synthons for various metal-containing materials.[28−35]

Two of the three nitrogen atoms in a 1,2,3-triazole ring are Lewis basic (Figure 1A),[36] and the C(5)−H bond (blue in Figure 1A) has been demonstrated as an effective hydrogen bond donor.[37−39] Therefore, the ability of hydrogen bond formation and metal coordination of the triazole ring can be explored for applications such as catalysis and sensing. Our group reported that fluorescent tetradentate ligands (e.g., **1** in Figure 1B) with high affinity for zinc ion (Zn^{2+}) can be assembled via the coupling between a fluorophore-appended azide and dipicolylamine-derivatized alkyne.[13] Compound **1** undergoes sensitive fluorescence enhancement under simulated physiological conditions in the presence of Zn^{2+}. The fluorescence enhancement was postulated to result from the termination of the non-radiative photoinduced electron transfer (PET) from the tertiary amino group to the excited 2-anthryltriazolyl fluorophore upon Zn^{2+} coordination.[40] In this Article, a detailed investigation on the coordination chemistry and photophysical processes embodied in compound **1** is described which reveals a relatively complete picture of the Zn^{2+}-coordination modulated fluorescence of **1**.

Results and Discussion

Ligands **1**−**5** (Figure 2) were prepared for this study. On the basis of our prior postulate, the tertiary amino group in **1** acts as the electron donor to the excited fluorophore during the PET quenching process. In compound **2** the tertiary amino group is eliminated so that the fluorescence of **2** is expected to be insensitive to the presence of Zn^{2+}.[41] In compound **3**, a tertiary amino group was incorporated without the pyridyl group. Therefore, the effect of the pyridyl group on the fluorescence can be extracted via comparison of the properties of **1** and **3**. In **4** and **5**, non-coordinating methyl and benzyl groups were included so that their effect on fluorescence could be examined. The syntheses of **1**−**5** are described in the Supporting Information.

X-ray Crystal Structure. The single crystals of the Zn^{2+} complex of **1** ($[Zn(\mathbf{1})(MeCN)](ClO_4)_2$) suitable for X-ray diffraction were grown via diffusion of diethyl ether into an MeCN solution of $[Zn(\mathbf{1})(MeCN)](ClO_4)_2$. The 2-anthryl and triazolyl groups are almost coplanar with a dihedral angle of 8.95°. Similar to the structures that we reported before,[13] the Zn^{2+} center adopts a trigonal bipyramidal geometry (Figure 3A). The two pyridyl and triazolyl groups occupy the equatorial sites whereas the tertiary amino group and a solvent molecule (MeCN) are found at the axial positions. The Zn−N3 bond length

(12) Struthers, H.; Mindt, T. L.; Schibli, R. *Dalton Trans.* **2010**, *39*, 675–696.
(13) Huang, S.; Clark, R. J.; Zhu, L. *Org. Lett.* **2007**, *9*, 4999–5002.
(14) David, O.; Maisonneuve, S.; Xie, J. *Tetrahedron Lett.* **2007**, *48*, 6527–6530.
(15) Schweinfurth, D.; Hardcastle, K.; Bunz, U. H. F. *Chem. Commun.* **2008**, 2203–2205.
(16) Tamanini, E.; Rigby, S. E. J.; Motevalli, M.; Todd, M. H.; Watkinson, M. *Chem.—Eur. J.* **2009**, *15*, 3720–3728.
(17) Komeda, S.; Lutz, M.; Spek, A. L.; Yamanaka, Y.; Sato, T.; Chikuma, M.; Reedijk, J. *J. Am. Chem. Soc.* **2002**, *124*, 4738–4746.
(18) Mindt, T. L.; Struthers, H.; Brans, L.; Anguelov, T.; Schweinsberg, C.; Maes, V.; Tourwe, D.; Schibli, R. *J. Am. Chem. Soc.* **2006**, *128*, 15096–15097.
(19) Maisonial, A.; Serafin, P.; Traïkia, M.; Debiton, E.; Théry, V.; Aitken, D. J.; Lemoine, P.; Viossat, B.; Gautier, A. *Eur. J. Inorg. Chem.* **2008**, 298–305.
(20) Struthers, H.; Spingler, B.; Mindt, T. L.; Schibli, R. *Chem.—Eur. J.* **2008**, *14*, 6173–6183.
(21) Mindt, T. L.; Schweinsberg, C.; Brans, L.; Hagenbach, A.; Abram, U.; Tourwé, D.; Garcia-Garayoa, E.; Schibli, R. *ChemMedChem* **2009**, *4*, 529–539.
(22) Chan, T. R.; Hilgraf, R.; Sharpless, K. B.; Fokin, V. V. *Org. Lett.* **2004**, *6*, 2853–2855.
(23) Liu, D.; Gao, W.; Dai, Q.; Zhang, X. *Org. Lett.* **2005**, *7*, 4907–4910.
(24) Detz, R. J.; Heras, S. A.; de Gelder, R.; van Leeuwen, P. W. N. M.; Hiemstra, H.; Reek, J. N. H.; van Maarseveen, J. H. *Org. Lett.* **2006**, *8*, 3227–3230.
(25) Bergbreiter, D. E.; Hamilton, P. N.; Koshti, N. M. *J. Am. Chem. Soc.* **2007**, *129*, 10666–10667.
(26) Bastero, A.; Font, D.; Pericàs, M. A. *J. Org. Chem.* **2007**, *72*, 2460–2468.
(27) Detz, R. J.; Delville, M. M. E.; Hiemstra, H.; van Maarseveen, J. H. *Angew. Chem., Int. Ed.* **2008**, *47*, 3777–3780.
(28) Diaz, D. D.; Punna, S.; Holzer, P.; McPherson, A. K.; Sharpless, K. B.; Fokin, V. V.; Finn, M. G. *J. Polym. Sci. A: Polym. Chem.* **2004**, *42*, 4392–4403.
(29) Li, Y.; Huffman, J. C.; Flood, A. H. *Chem. Commun.* **2007**, 2692–2694.
(30) Meudtner, R. M.; Ostermeier, M.; Goddard, R.; Limberg, C.; Hecht, S. *Chem.—Eur. J.* **2007**, *13*, 9834–9840.
(31) Camp, C.; Dorbes, S.; Picard, C.; Benoist, E. *Tetrahedron Lett.* **2008**, *49*, 1979–1983.
(32) Badèche, S.; Daran, J.-C.; Ruiz, J.; Astruc, D. *Inorg. Chem.* **2008**, *47*, 4903–4908.
(33) Schulze, B.; Friebe, C.; Hager, M. D.; Winter, A.; Hoogenboom, R.; Görls, H.; Schubert, U. S. *Dalton Trans.* **2009**, 787–794.
(34) Demessence, A.; D'Alessandro, D. M.; Foo, M. L.; Long, J. R. *J. Am. Chem. Soc.* **2009**, *131*, 8784–8786.
(35) Crowley, J. D.; Bandeen, P. H. *Dalton Trans.* **2010**, *39*, 612–623.
(36) Brotherton, W. S.; Michaels, H. A.; Simmons, J. T.; Clark, R. J.; Dalal, N. S.; Zhu, L. *Org. Lett.* **2009**, *11*, 4954–4957.
(37) Li, Y.; Flood, A. H. *Angew. Chem., Int. Ed.* **2008**, *47*, 2649–2652.
(38) Li, Y.; Flood, A. H. *J. Am. Chem. Soc.* **2008**, *130*, 12111–12122.
(39) Juwarker, H.; Lenhardt, J. M.; Pham, D. M.; Craig, S. L. *Angew. Chem., Int. Ed.* **2008**, *47*, 3740–3743.
(40) de Silva, A. P.; Gunaratne, H. Q. N.; Gunnlaugsson, T.; Huxley, A. J. M.; McCoy, C. P.; Rademacher, J. T.; Rice, T. E. *Chem. Rev.* **1997**, *97*, 1515–1566.
(41) Zhu, L.; Zhang, L.; Younes, A. H. *Supramol. Chem.* **2009**, *21*, 268–283.

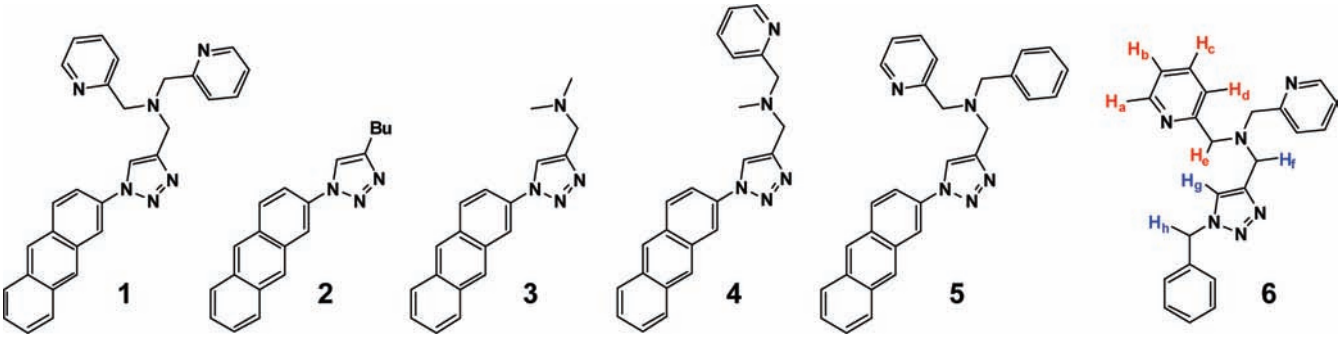

Figure 2. Structures of compounds **1**−**6**. The labeling of hydrogens in **6** is to facilitate the presentation of the ^{1}H NMR titration data shown in Figure 7. The hydrogens coded red are associated with the pyridyl groups; the hydrogens coded blue are associated with the triazolyl moiety.

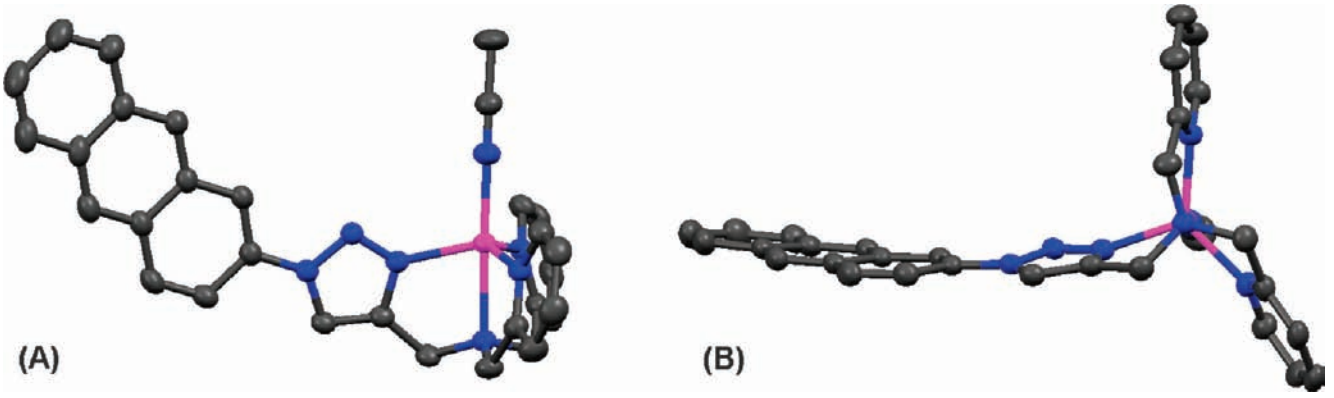

Figure 3. (A) X-ray crystal structure (50% probability ellipsoids) of $[Zn(\mathbf{1})(MeCN)]^{2+}$. MeCN: acetonitrile. The omitted counterion is perchlorate; (B) the view down the dative bond between the tertiary amino group and the Zn^{2+} center reveals a propeller-like conformation.

(2.032 Å) is similar to the lengths of dative bonds between Zn^{2+} and pyridyl nitrogen atoms (2.035 Å and 2.059 Å). Looking down the dative bond between the tertiary amino group and Zn^{2+}, a propeller-like conformation is identified (Figure 3B) which resembles the structures of other tetradentate Zn^{2+} complexes in the literature.[42−44] The crystal structure of $[Zn(\mathbf{1})(MeCN)](ClO_4)_2$ suggests a 1:1 binding stoichiometry.

Cyclic Voltammetry (CV) Studies. Compound **1** undergoes irreversible electrochemical oxidation as shown in the cyclic voltammogram (black, Figure 4). The anodic peak with lower potential was assigned to the tertiary amino group (1.03 V vs Ag/AgCl) and the one with higher potential was attributed to the oxidation of the 2-anthryltriazolyl fluorophore (1.44 V). The assignment was based on the comparison of the cyclic voltammogram of **1** with those of compounds **2** and **3**. Compound **2** (blue, Figure 4) shows only the anodic peak of the fluorophore because of the absence of the tertiary amino group. Similar to compound **1**, compound **3** (red, Figure 4) displays both bands. The higher oxidation potential of the tertiary amino group than that of the 2-anthryltriazolyl fluorophore renders the photoinduced electron transfer (PET) processes in the excited **1** and **3** thermodynamically favorable.[45] This competing

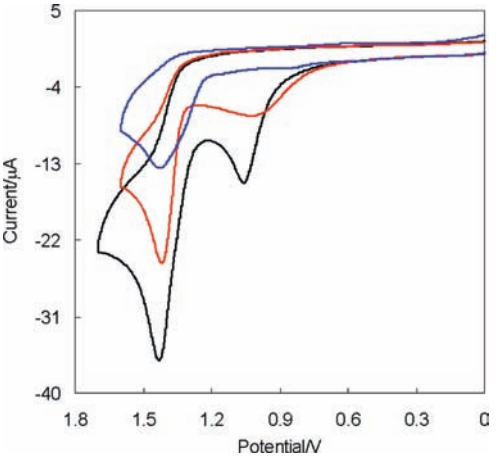

Figure 4. Cyclic voltammograms of **1** (black, E_{pa} = 1.03 V, 1.44 V), **2** (blue, E_{pa} = 1.49 V), and **3** (red, E_{pa} = 0.98 V, 1.42 V) in MeCN. Bu_4NPF_6 (0.1 M) was used as the supporting electrolyte. Working electrode: glassy carbon electrode; reference electrode: Ag/AgCl. Scan rate: 0.1 V/s.

relaxation pathway diminishes the fluorescence quantum yield of the fluorophore. The 1:1 binding stoichiometry revealed by the X-ray crystal structure of the Zn^{2+} complex of **1** and the thermodynamic feasibility for PET in **1** suggested by the CV data lends support to the interpretation that the formation of the 1:1 Zn^{2+} complex results in fluorescence enhancement because of the blockage of the fluorescence quenching PET process in **1**.

Isothermal Titration Calorimetry (ITC) Studies. The coordination between Zn^{2+} and **1** in MeCN was further

(42) Allen, C. S.; Chuang, C.-L.; Cornebise, M.; Canary, J. W. *Inorg. Chim. Acta* **1995**, *239*, 29–37.
(43) Zhu, L.; dos Santos, O.; Koo, C. W.; Rybstein, M.; Pape, L.; Canary, J. W. *Inorg. Chem.* **2003**, *42*, 7912–7920.
(44) Royzen, M.; Durandin, A.; Young, V. G. J.; Geacintov, N. E.; Canary, J. W. *J. Am. Chem. Soc.* **2006**, *128*, 3854–3855.
(45) Zhang, L.; Zhu, L. *J. Org. Chem.* **2008**, *73*, 8321–8330.

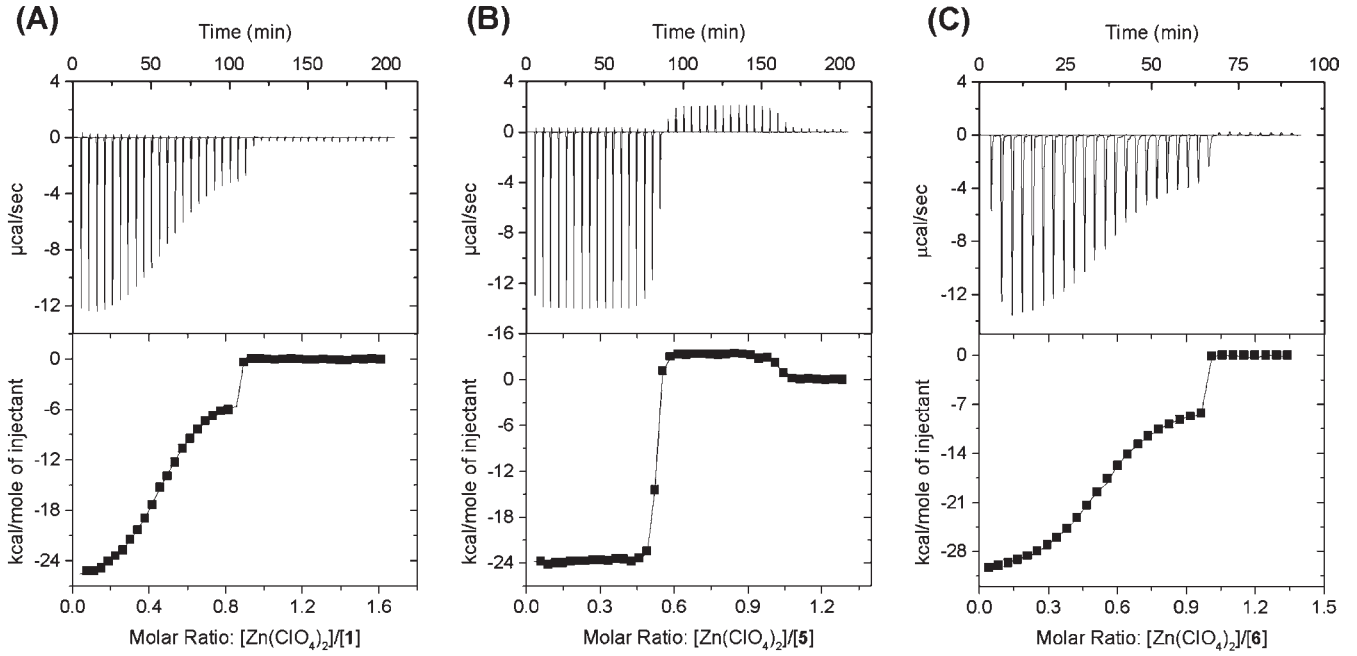

Figure 5. ITC titrations of (A) **1** (0.20 mM) with $Zn(ClO_4)_2$ (1.8 mM), $n_1 = 0.431$, $\Delta H°_1 = -27.3$ kcal/mol, $n_2 = 0.422$, $\Delta H°_2 = -3.88$ kcal/mol; (B) **5** (0.36 mM) with $Zn(ClO_4)_2$ (2.6 mM), $n_1 = 0.513$, $\Delta H°_1 = -23.8$ kcal/mol, $n_2 = 0.494$, $\Delta H°_2 = 2.39$ kcal/mol; (C) **6** (0.30 mM) with $Zn(ClO_4)_2$ (1.8 mM), $n_1 = 0.496$, $\Delta H°_1 = -32.3$ kcal/mol, $n_2 = 0.469$, $\Delta H°_2 = -6.17$ kcal/mol.

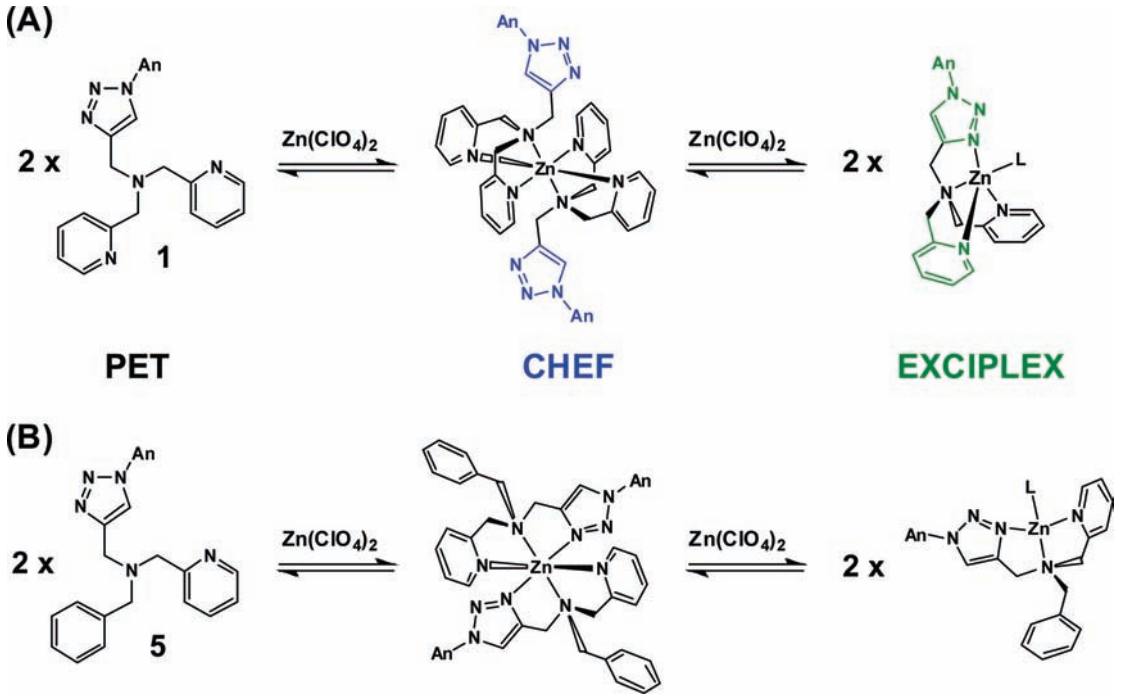

Figure 6. Postulated two-step binding processes of (A) **1** and (B) **5** with $Zn(ClO_4)_2$. The photophysical consequence in each step of (A) is discussed later in the text. An: 2-anthryl; PET: photoinduced electron transfer; CHEF: chelation-enhanced fluorescence.

investigated via isothermal titration calorimetry (ITC).[45] Contrary to a 1:1 binding model that one might expect based on the X-ray crystal structure, two thermally distinct processes were identified as $Zn(ClO_4)_2$ was titrated into a solution of **1** (Figure 5A). The first thermal transition occurs at a molar ratio of ~0.5, suggesting a 2:1 (ligand: Zn^{2+}) complex (Figure 6A). The second step completes a 1:1 complex. The exothermicity of both steps may have resulted from the formation of strong dative bonds between the pyridyl or triazolyl moieties with Zn^{2+} relative to the solvation energy of Zn^{2+} in MeCN.[46] Compound **6**,[13] which has a benzyl group attached to the triazole ring, displays a similar ITC trace to that of **1** (Figure 5C).

The tridentate ligand **5** also shows a two-step binding process with Zn^{2+} (Figure 5B). The first step to afford the

(46) Younes, A. H.; Zhang, L.; Clark, R. J.; Zhu, L. *J. Org. Chem.* **2009**, *74*, 8761–8772.

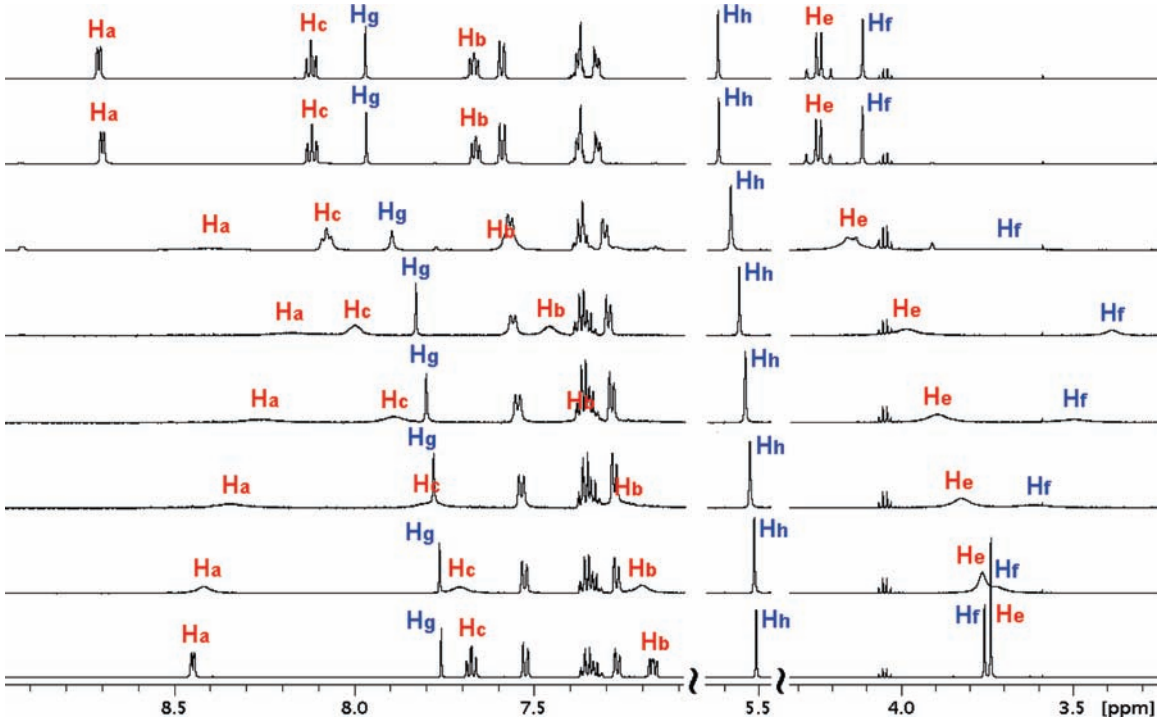

Figure 7. Partial ^{1}H NMR spectra (500 MHz, CD_3CN) of **6** in the presence of increasing concentrations of $Zn(ClO_4)_2$ (bottom to top: [Zn]/[**6**] = 0, 0.05, 0.14, 0.24, 0.35, 0.59, 0.83, 1.06). The quartet at 4.05 ppm results from the residual ethyl acetate in the sample.

presumed 2:1 complex is exothermic; however, the second step to reach the 1:1 complex is slightly endothermic. As shown in Figure 6B, the conversion from the 2:1 to the 1:1 complex does not involve making or breaking the N−Zn dative bonds. Therefore, the thermal effect of the second step is expected to be small and either endo- or exothermic.[46]

^{1}H NMR Titration Studies. The ^{1}H NMR of compound **6** in CD_3CN changes with the addition of $Zn(ClO_4)_2$ as a result of coordination (Figure 7). The peaks were assigned based on the 2D-COSY experiments (Supporting Information, Figure S9). Most hydrogens on **6** (e.g., H_b, H_c, H_e, H_g, and H_h, see labeling in Figure 2) undergo downfield shifts as the deshielding Zn^{2+} is incorporated to form the complex. H_a and H_f, however, undergo upfield shifts with the initial addition of $Zn(ClO_4)_2$ before turning back downfield during the latter half of the titration. Evidently, a simple two-species interconversion between the free ligand of **6** and its 1:1 Zn^{2+} complex is not sufficient to explain the two-step changes that H_a and H_f experienced during the titration experiment.

The dependence of normalized chemical shifts ($\delta_n = (\delta - \delta_{min})/(\delta_{max} - \delta_{min})$) of selected hydrogens on the molar ratio of **6** and $Zn(ClO_4)_2$ ([Zn]/[**6**]) leads to more insight in the chemical events taking place during the titration experiment (Figure 8). The color coding scheme reflects the assignment shown in Figure 2, where hydrogens in red and blue are primarily associated with the pyridyl groups and the triazolyl group, respectively. Three groups of hydrogens are identified in Figure 8. The chemical shifts of H_b, H_c, and H_e (red in the top portion of Figure 8) increase slightly more rapidly during the first leg of the titration than those of the hydrogens associated with the triazolyl group (e.g., H_g and H_h, blue in the middle portion of Figure 8). This observation is consistent with the hypothesis that binding between Zn^{2+} and the triazolyl

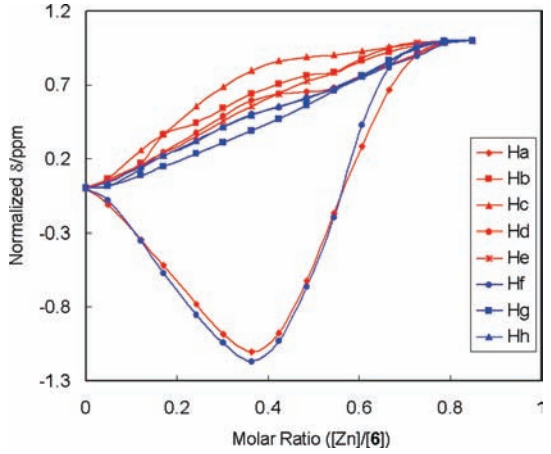

Figure 8. Normalized chemical shifts ($\delta_n = (\delta - \delta_{min})/(\delta_{max} - \delta_{min})$) of hydrogen atoms versus the molar ratio of $Zn(ClO_4)_2$ and **6** in CD_3CN. Hydrogens coded red and blue are considered as "associated with" the pyridyl groups and the triazolyl groups, respectively (see assignment in Figure 2).

group occurs after that of the pyridyl groups. The fact that H_a and H_f (the bottom group) first undergo significant upfield shifts can be explained by the 2:1 complex structure in Figure 6A (with benzyl replacing the 2-anthryl group). H_a might be close enough to the phenyl ring to experience the shielding ring current, while H_f (the CH_2 between the triazolyl group and the tertiary nitrogen) might be situated on top of the pyridyl ring to be shielded as well. The 1:1 complex formation removes all the shielding ring currents, which consequently leads to downfield shifts of H_a and H_f.

The significant line-broadening of the hydrogens that are associated with the dipicolylamino group (coded red in Figure 7 and H_f) suggests that the coordination dynamics

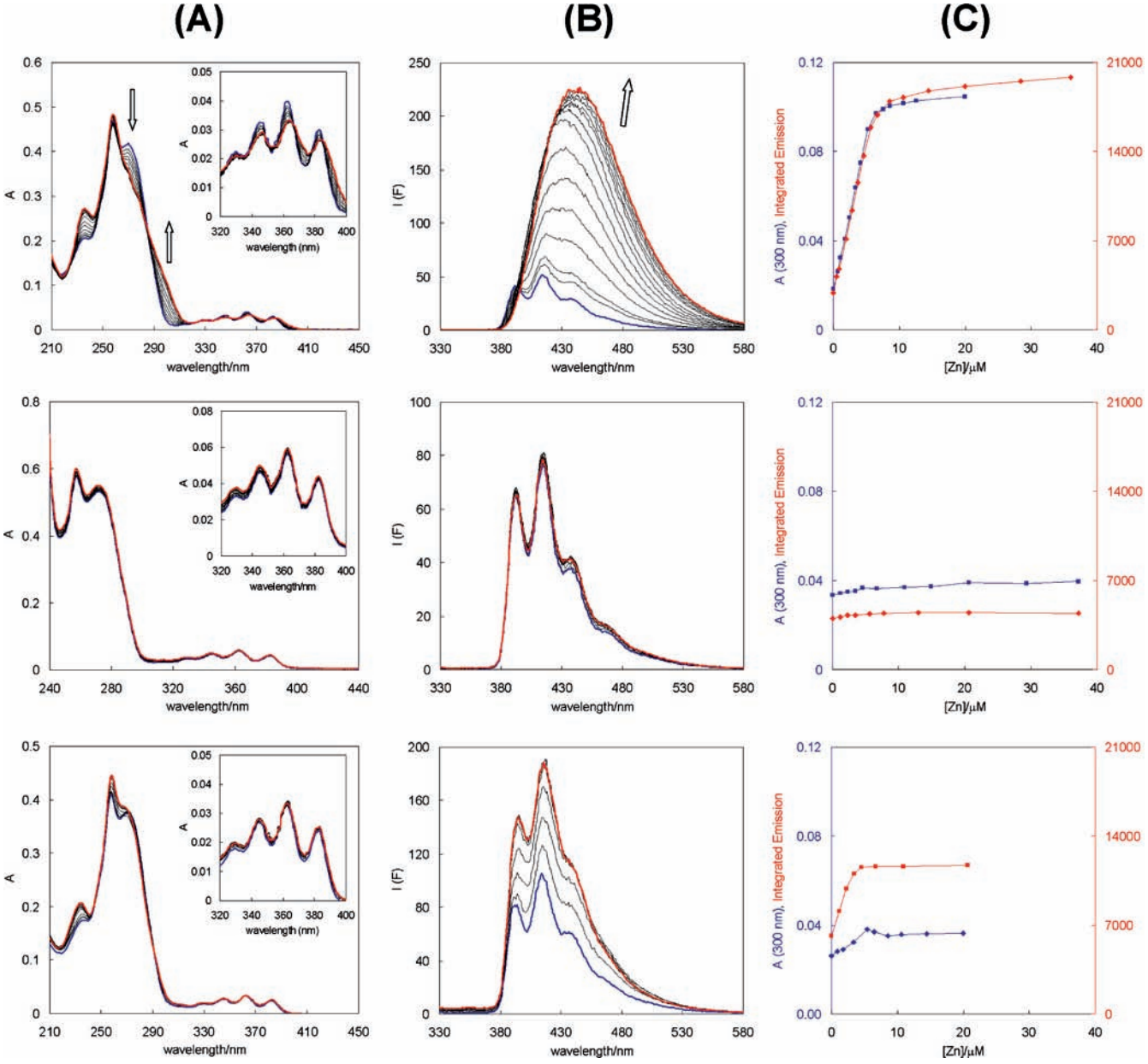

Figure 9. Absorption (A) and fluorescence (B, λ_{ex} = 300 nm) titration profiles of compounds **1** (6.9 μM, top row), **2** (7.5 μM, middle), and **3** (7.1 μM, bottom) with $Zn(ClO_4)_2$ with MeCN. The spectra of free ligands and Zn^{2+} complexes at saturation levels are coded blue and red, respectively; (C) absorbance values at 300 nm (blue) and integrated fluorescence (red) vs [Zn].

between Zn^{2+} and the dipicolylamino group is on the time scale of the ^1H NMR experiment. By comparison, the lack of line-broadening of H_g and H_h, both of which are associated with the triazolyl group and are not affected by the dipicolylamino binding as much as the other hydrogens, suggests faster binding dynamics between Zn^{2+} and the triazolyl group than that between Zn^{2+} and the dipicolylamino group. Detailed kinetic studies will be carried out using variable temperature analysis.

Absorption Titration Studies in Acetonitrile. The absorption spectrum of **1** undergoes Zn^{2+}-dependent shifts (Figure 9A, top row). The vibronic bands of the anthryl group undergo an overall bathochromic shift with addition of Zn^{2+}. The isosbestic points were observed at 285, 366, 378, and 385 nm. The more pronounced changes come at the range of 260−310 nm with an isosbestic point at 285 nm. The appearance of isosbestic points suggests an interconversion between two species—free ligand and its Zn^{2+} complex. However, when three species are involved in the equilibrium as postulated in Figure 6A, as long as two of the three species have coincidentally similar absorption spectra (e.g., the 2:1 and 1:1 complexes), isosbestic points may result.

Fluorescence Titration Studies in Acetonitrile. Excited at 300 nm, the structured fluorescence spectrum of **1** (Figure 9B, top row, blue) shows an initial moderate enhancement of intensity followed by the bathochromic shift to an unstructured band with much higher intensity in the presence of increasing amount of Zn^{2+}.[47] By

(47) Excitation at 357 nm resulted in similar observations: the fluorescence profile of **1** of the Zn^{2+}-titration experiment is consistent with a two-step Zn^{2+}-binding process. The molar absorptivity of the Zn^{2+} complex of **1** at 300 nm, however, is much larger than that at 357 nm, which accounts for the difference of emission intensity of two fluorescence titration profiles (Supporting Information, Figure S1).

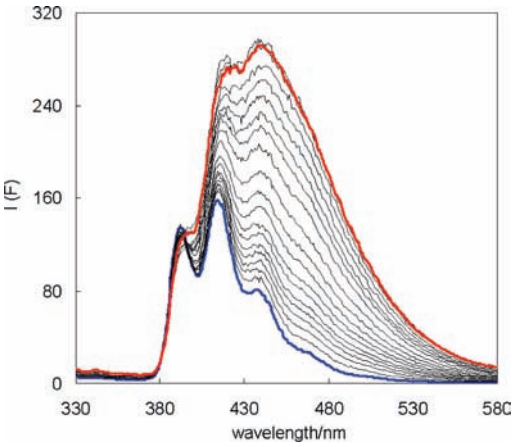

Figure 10. Fluorescence titration profile (λ_{ex} = 300 nm) of compound **2** (10 μM), pyridine (42 mM), and $Zn(ClO_4)_2$ (0−26 mM) in MeCN.

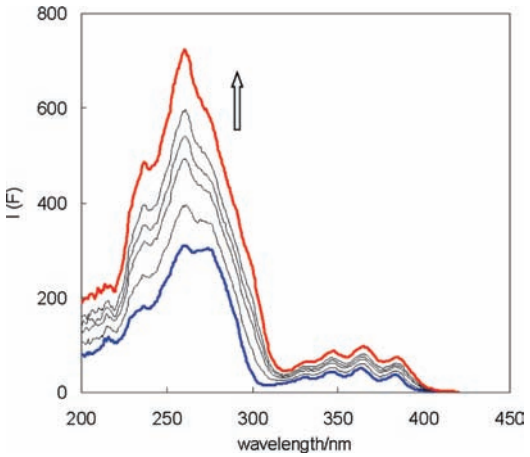

Figure 11. Fluorescence excitation spectra of **1** (9.1 μM, λ_{em} = 430 nm) in the presence of $Zn(ClO_4)_2$ (0−10 μM) in MeCN. Blue and red spectra were taken at [Zn] = 0 and 10 μM, respectively.

replacing the dipicolylamino group with the *n*-butyl group, the fluorescence of compound **2** shows little change in the presence of Zn^{2+} (Figure 9B, middle). This observation supports the postulate that PET from the tertiary amino group to the excited fluorophore is operating in **1** in the absence of Zn^{2+}. When a tertiary amino group is restored to afford **3**, a moderate fluorescence enhancement caused by the addition of Zn^{2+} was indeed observed, however, without further shifting to a longer, unstructured emission band (Figure 9B, bottom). Clearly, the formation of the low-energy, unstructured band is the result of the interactions between the pyridyl groups and the excited fluorophore in the Zn^{2+} complex of **1**.[48] The involvement of the pyridyl group is further supported by the fluorescence titration data of compounds **4** and **5** with $Zn(ClO_4)_2$ where both pyridyl-containing ligands are capable of generating the long, unstructured bands with the addition of Zn^{2+} (Supporting Information, Figures S3 and S4). The unstructured bands at long wavelengths are attributed to the emission from an intramolecular exciplex between the excited fluorophore and the zinc-bound pyridyl group, where a charge-transfer process might occur from the excited 2-anthryltriazolyl group to the zinc-bound pyridyl group in the excited state.[49] Although the complex is preformed in the ground state, we still describe the excited state structure as an "intramolecular exciplex" because of the apparent lack of mirror image relationship between its excitation (Figure 11) and emission spectra. The interaction between the 2-anthryltriazolyl and zinc-bound pyridyl groups resulting in the low energy structureless emission band does not occur until the 2-anthryltriazolyl group is excited.

To test the hypothesis that the appearances of the structureless emission bands of **1**, **4**, and **5** during the latter half of Zn^{2+} titration experiments are due to the formation of exciplexes between the 2-anthryltriazolyl group and the Zn^{2+}-bound pyridyl group, $Zn(ClO_4)_2$ was titrated into a mixture of compound **2** and pyridine. A red-shifted structureless band (Figure 10) evolves as Zn^{2+} concentration increases, which is presumably originated from the ternary exciplex between **2**, pyridine, and Zn^{2+}. Also consistent with the interpretation invoking an intramolecular exciplex, the excitation spectra of **1** collected in the presence of Zn^{2+} of various concentrations (Figure 11) resemble its absorption spectra and lack the mirror image relationship with its emission spectra. This observation indicates that electronic structural changes of the excited state have occurred prior to emission.

Lifetimes and Fluorescence Quantum Yields of Ligands and Their Zn^{2+} Complexes. The fluorescence quantum yields (ϕ_f) of all ligands but **2** increase upon Zn^{2+} complex formation (Table 1). The coordination at the tertiary amino groups in **1** and **3**−**5** shuts down the PET pathway, which restores the fluorescence. Ligand **2** shows a single-exponential decay determined by the time-correlated single photon counting (TCSPC) method,[50] whereas other ligands show biexponential decays (Table 1). The slow components in ligands **1** and **3**−**5** (3.4−4.7 ns) can be assigned to the decay of the 2-anthryltriazolyl fluorophore; which are similar in magnitude to that of **2**. The fast components (1.8−2.7 ns), on the other hand, can be assigned to the excited species accessible to the PET decay pathway. When Zn^{2+} coordinates, the PET pathways are being slowed down. Consequently, the fast components between 2 and 3 ns in ligands **1** and **3**−**5** disappear. The Zn^{2+} complex of **3**, which does not contain a pyridyl group, displays a single exponential (4.9 ns) attributable to the decay of the fluorophore. For pyridyl-containing ligands **1**, **4**, and **5**, on the other hand, new, slow components ~8 ns appear upon Zn^{2+} coordination. These slow components are assigned to the emission of the intramolecular exciplexes between the excited fluorophore and the Zn^{2+}-bound pyridyl groups (see similar examples in Figure 12). Consistent with the intramolecular exciplex formation hypothesis, the abundance of the slow component of **1** grows from 69% to 82% when the emission wavelength monitored in the TCSPC experiments increases from 400 to

(48) The intramolecular nature of the formation of the bathochromically shifted emission band is supported by the dilution experiment of the Zn^{2+} complex of **1** described in the Supporting Information, Figure S2. A similar emission band resulted from the ternary complex of **2**, pyridine, and Zn^{2+} requires high pyridine and $Zn(ClO_4)_2$ concentrations (at millimolar, see Figure 10), which further discounts the possibility that the bathochromically shifted emission band of $[Zn(\mathbf{1})]^{2+}$ is resulted from diffusion-controlled intermolecular interactions.

(49) Beens, H.; Knibbe, H.; Weller, A. *J. Chem. Phys.* **1967**, *47*, 1183–1185.

(50) Lakowicz, J. R. In *Principles of Fluorescence Spectroscopy*, 3rd ed.; Springer: New York, 2006; pp 103−107.

Table 1. Fluorescence Quantum Yields (ϕ_f), Lifetimes (τ, λ_{ex} = 370 nm),[a] and χ^2 of **1**−**5** and Their Zn^{2+} Complexes in MeCN

	1	[Zn(**1**)]	**2**	[Zn(**2**)]	**3**	[Zn(**3**)]	**4**	[Zn(**4**)]	**5**	[Zn(**5**)]
ϕ_f	0.17	0.36	0.24	0.26	0.17	0.27	0.18	0.40	0.16	0.43
τ_1	4.43 (36%)	5.08 (33%)	4.70	4.78	4.49 (40%)	4.89	4.45 (49%)	4.68 (36%)	3.41 (78%)	3.70 (19%)
τ_2	2.72 (64%)	8.09 (67%)	N. A.	N. A.	2.66 (60%)	N. A.	2.67 (51%)	8.49 (64%)	1.81 (22%)	7.36 (81%)
χ^2	0.57	1.02	0.90	1.12	0.73	1.24	0.90	1.10	0.90	1.21

[a] Fluorescence decay traces of free ligands and Zn^{2+} complexes were observed at 415 and 440 nm, respectively. The relative abundances of individual exponentials are in the parentheses.

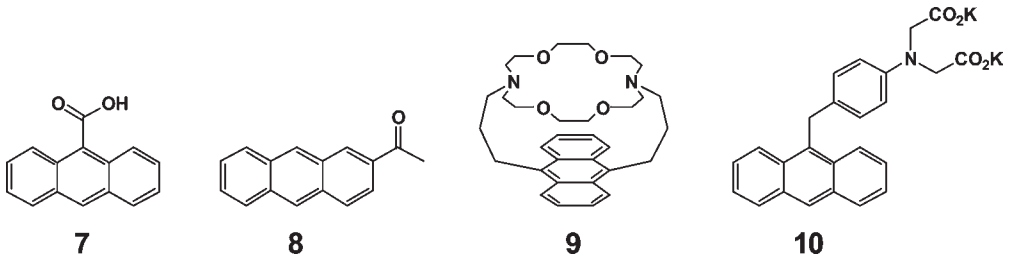

Figure 12. Examples in which either a charge transfer process and/or an "intramolecular exciplex" formation involving an excited anthryl group was invoked.

480 nm. Transient fluorescence spectroscopy with better time resolution will be carried out in the future to delineate the kinetics of exciplex formation of **1**.

The structureless emission bands from anthracene derivatives have been observed on several occasions. Compound **7** (Figure 12), studied by Werner et al., shows only a structureless emission band at lower energy than that of the parent anthracene emission in MeCN, benzene, and acidified MeOH.[51] It was concluded that the charge transfer from the excited 9-anthryl group to the carboxyl group (−COOH), which is accompanied by a conformational change of the molecule, produces a highly dipolar excited state. This charge-transfer process generates "a sort of intramolecular exciplex"[52] between the anthryl moiety and the carboxyl group. Similar to **7**, compound **8** displays rounded, low-energy emission in the presence of alcohol.[53−55] Presumably hydrogen-bonding between the carbonyl and the alcohol additive facilitates charge transfer from the excited 2-anthryl to the carbonyl to result in a relaxed excited state analogous to an intramolecular exciplex. In compounds **7** and **8**, the coplanarity between the putative electron donor (anthryl) and acceptor (carboxyl or carbonyl) can be achieved in either the excited or the ground states. One can simply invoke the concept of internal charge transfer (ICT)[41] to explain the formation of the structureless emission bands and their solvent dependence. The observations of the next two examples, on the other hand, are more relevant to what we detected in the current study.

The anthraceno-cryptand **9** displays low energy structureless emission bands. These signals are most abundant in aprotic solvents such as MeCN.[56] Such emission was ascribed to the intramolecular exciplex between the two amino groups and the excited anthryl group, where the electron density shifts from the amino groups to the excited anthryl component.[57] Consistent with the exciplex hypothesis, when metal ions with matching sizes to the azacrown are added, the exciplex emission is displaced by a typical structured anthryl emission at a higher energy.[58] In the recent work on **10** by Gunnlaugsson et al., the formation of a Zn^{2+} complex in an aqueous buffer elicits an exciplex-like emission.[59]

On the basis of the observations on our systems and related literature reports, the model shown in Figure 6A is established. When compound **1** is in the presence of Zn^{2+} at a low concentration, a 2:1 complex (ligand to Zn^{2+}) where the triazolyl group is uncoordinated may dominate. The coordination at the tertiary amino group mitigates the PET process to result in a moderate fluorescence enhancement (a CHEF effect). When the Zn^{2+} concentration is high, the 1:1 complex becomes abundant. The coordination of the triazolyl group reduces the net distance between the Zn^{2+}-bound pyridyl and the 2-anthryltriazolyl group; therefore, an intramolecular exciplex formation is enabled where the transfer of electron density from the 2-anthryltriazolyl component to the Zn^{2+}-bound pyridyl occurs in the excited state. Low-energy, structureless emission was recorded in both aprotic (MeCN) and protic (aqueous, Figure 13A) solvents, however with little solvent dependence. The lack of solvent dependence of the "exciplex" emission[49] of the Zn^{2+}-complex of **1** may be attributed to the dominating stabilizing effect of Zn^{2+} exerted on the excited state, which diminishes the effect of solvent polarity on the excited state. Similar observations were made by us on other complexes between Zn^{2+} and charge-transfer type of fluoroionophores.[46] The elevated fluorescence quantum yield of

(51) Werner, T. C.; Hercules, D. M. *J. Phys. Chem.* **1969**, *73*, 2005–2011.
(52) Suppan, P.; Ghoneim, N. In *Solvatochromism*; The Royal Society of Chemistry: Cambridge, U.K., 1997; p 119.
(53) Tamaki, T. *Bull. Chem. Soc. Jpn.* **1980**, *53*, 577–582.
(54) Tamaki, T. *Bull. Chem. Soc. Jpn.* **1982**, *55*, 1756–1760.
(55) Tamaki, T. *Bull. Chem. Soc. Jpn.* **1982**, *55*, 1761–1767.
(56) Konopelski, J. P.; Kotzyba-Hibert, F.; Lehn, J.-M.; Desvergne, J.-P.; Fagès, F.; Castellan, A.; Bouas-Laurent, H. *J. Chem. Soc., Chem. Commun.* **1985**, 433–436.
(57) Fagès, F.; Desvergne, J.-P.; Bouas-Laurent, H. *J. Am. Chem. Soc.* **1989**, *111*, 96–102.
(58) Fagès, F.; Desvergne, J.-P.; Bouas-Laurent, H.; Marsau, P.; Lehn, J.-M.; Kotzyba-Hibert, F.; Albrecht-Gary, A.-M.; Al-Joubbeh, M. *J. Am. Chem. Soc.* **1989**, *111*, 8672–8680.
(59) Gunnlaugsson, T.; Lee, T. C.; Parkesh, R. *Tetrahedron* **2004**, *60*, 11239–11249.

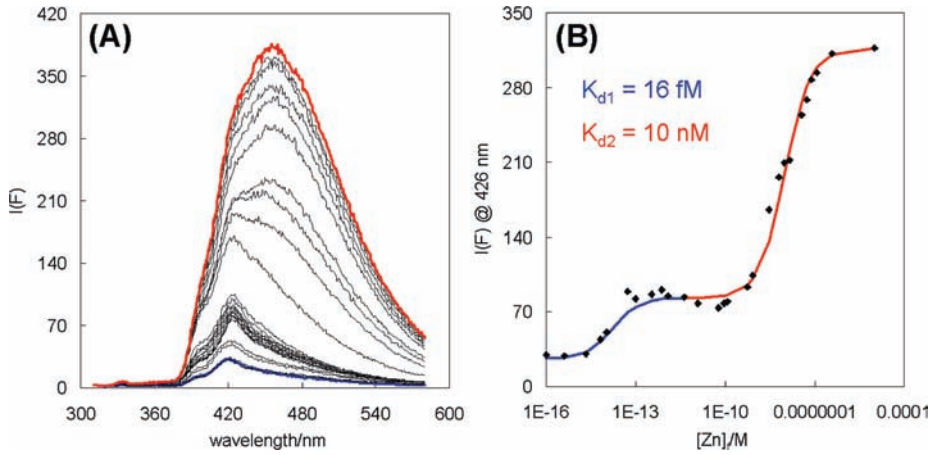

Figure 13. (A) Fluorescence spectra of **1** (20 μM, λ_{ex} = 300 nm) in the presence of $Zn(ClO_4)_2$ (0−10 mM) in an aqueous solution ([HEPES] = 50 mM, [KNO_3] = 100 mM, [EDTA] = 5 mM, [EGTA] = 5 mM, pH = 7.2). The spectra in the absence of Zn^{2+} and in the presence of 10 mM of Zn^{2+} are coded blue and red, respectively. (B) Fluorescence intensity at 426 nm vs the concentrations of free Zn^{2+}. Blue and red lines are theoretical fitting curves based on a 1:1 binding model.

the exciplex may be partly due to the reduced degree of freedom of the 1:1 complex relative to those of the free ligand and the 2:1 complex.[46]

Fluorescence Titration Studies in an Aqueous Buffer. The Zn^{2+} titration experiment in a neutral aqueous solution was reexamined in light of the two-step binding process discovered in MeCN. Two metal ion chelators, EDTA and EGTA, were included in the buffer solution to control the free Zn^{2+} concentrations.[60] When excited at 300 nm, compound **1** shows weak fluorescence (blue spectrum in Figure 13A). An enhancement is followed with the addition of Zn^{2+}. With sufficient amount of Zn^{2+} added, a broader emission band centered at 460 nm starts to appear, which is further enhanced as the titration continues. On the basis of the amount of total Zn^{2+} added at each titration and the concentrations of the metal chelators, the concentrations of free Zn^{2+} were calculated using the tool "Webmaxc Standard".[60,61] The fluorescence intensity at 426 nm was plotted against the free Zn^{2+} concentrations and revealed a two-step process (Figure 13B). By fitting each step with a 1:1 binding equation,[62] the "apparent" 1:1 dissociation constants (K_d) to Zn^{2+} that ligand **1** displays at the early and late stages of the titration are 16 fM and 10 nM, respectively.

The fluorescence titration studies of **1** with Ca^{2+}, Cu^{2+}, and Cd^{2+} under the neutral aqueous conditions were studied. As a typical polyaza ligand, **1** is expected to bind divalent transition metal ions with high affinities. Cu^{2+} was chosen as a representative first-row paramagnetic transition metal ion. The coordination between Cu^{2+} and **1** is evident by the extremely high apparent 1:1 dissociation constant of 0.03 fM. As a paramagnetic metal ion, Cu^{2+} quenches the fluorescence of **1** effectively (Supporting Information, Figure S5). Cd^{2+}, which along with Zn^{2+} belongs to Group 2B, enhances the fluorescence of **1**. However, the emission band of the Cd^{2+} complex centers at 430 nm, shorter than that of the Zn^{2+} complex (Supporting Information, Figure S6). Furthermore, the fluorescence binding isotherm of Cd^{2+} titration is not fittable with the 1:1 binding equation, which suggests that Cd^{2+} binds to **1** with a different geometry and/or stoichiometry from that of Zn^{2+}. Ca^{2+}, which is one of the likely interfering metal ions in live-cell imaging experiments, does not alter the fluorescence of **1** (Supporting Information, Figure S7). The non-interference from the biologically abundant metal ions such as Ca^{2+} and Mg^{2+} is a prerequisite for a fluorescent ligand to be used in live-cell imaging applications.[13] In the next section, the preliminary study of **1** as a potential fluorescent indicator for Zn^{2+} in live-cell imaging applications[63−66] is presented.

Live-Cell Fluorescence Imaging Studies. The fluorescence of compound **1** undergoes a significant enhancement upon Zn^{2+} coordination in buffered aqueous conditions (Figure 13). Also, it shows superior selectivity for Zn^{2+} over other abundant metal ions in biological systems such as Ca^{2+} and Mg^{2+}. Herein, we report the preliminary evaluation of the potential of **1** in live-cell imaging of Zn^{2+}. Compound **1** permeates into HeLa (CCL2 line) cells readily upon incubation for 30 min. Cells loaded with **1** do not show morphological changes over 2−3 h which indicates that the adverse effect of **1** is not significant over the time scales of most fluorescence imaging experiments. Upon further incubation of indicator-loaded cells in the presence of 20 μM of TPEN, a strong membrane-permeable Zn^{2+} chelator,[67] to create a Zn^{2+}-deprived condition, weak fluorescence was observed (Figure 14A) after an extra 10 min incubation. If 100 μM $ZnCl_2$ was added to afford a Zn^{2+}-rich environment, a fluorescence enhancement is evident after 10 min incubation (Figure 14B). The physiological compatibility of **1** and its effectiveness to signal the presence of Zn^{2+} via fluorescence enhancement provide motivation for us to make structural alterations of this ligand to optimize its performance as a legitimate intracellular fluorescent indicator for Zn^{2+}.

(60) Zhang, L.; Murphy, C. S.; Kuang, G.-C.; Hazelwood, K. L.; Constantino, M. H.; Davidson, M. W.; Zhu, L. *Chem. Commun.* **2009**, 7408–7410.
(61) Patton, C.; Thompson, S.; Epel, D. *Cell Calcium* **2004**, *35*, 427–431.
(62) Tsien, R. Y.; Pozzan, T.; Rink, T. J. *J. Cell. Biol.* **1982**, *94*, 325–334.
(63) Kikuchi, K.; Komatsu, H.; Nagano, T. *Curr. Opin. Chem. Biol.* **2004**, *8*, 182–191.
(64) Thompson, R. B. *Curr. Opin. Chem. Biol.* **2005**, *9*, 526–532.
(65) Dai, Z.; Canary, J. W. *New J. Chem.* **2007**, *31*, 1708–1718.
(66) Nolan, E. M.; Lippard, S. J. *Acc. Chem. Res.* **2009**, *42*, 193–203.
(67) Arslan, P.; Virgilio, F. D.; Beltrame, M.; Tsien, R. Y.; Pozzan, T. *J. Biol. Chem.* **1985**, *260*, 2719–2727.

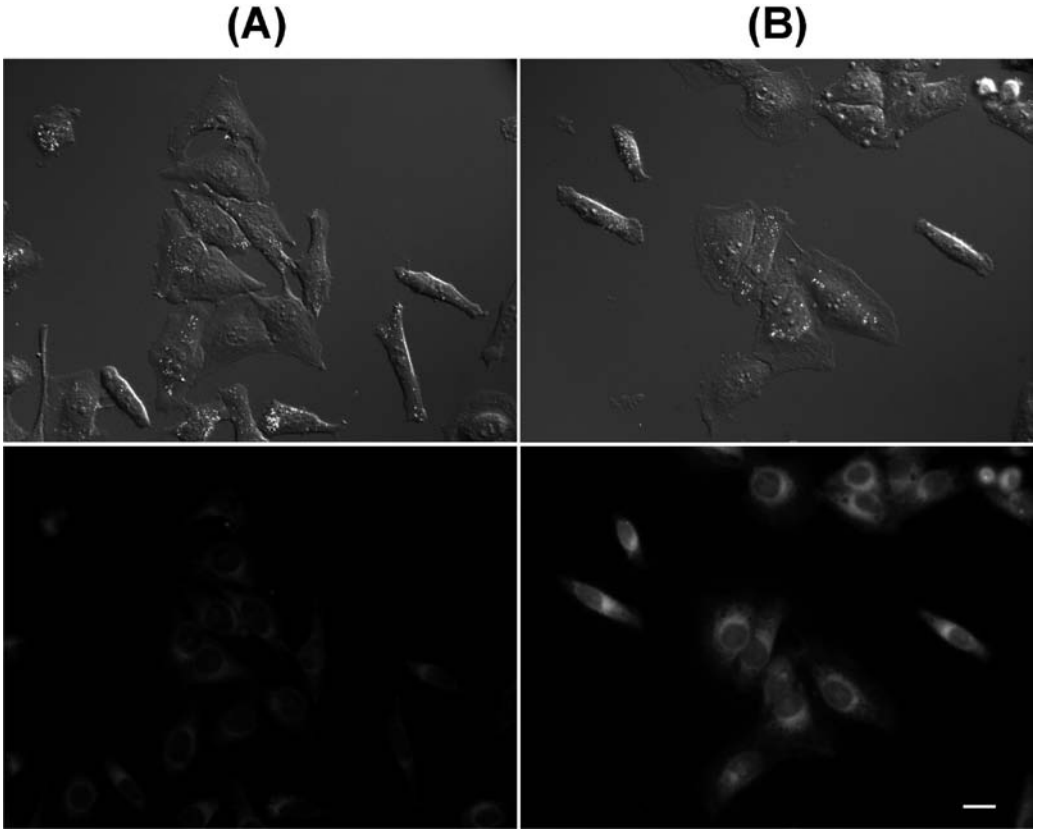

Figure 14. Differential interference contrast (DIC, upper) and fluorescence (lower) images of live HeLa cells (37 °C, 5% CO_2) after incubation in DMEM culture media with **1** (20 μM, 30 min). Cells were then incubated in the presence of 20 μM TPEN and 100 μM sodium pyrithione in HBSS buffer for an additional 10 min with (A) no zinc added, and (B) in the presence of 100 μM $ZnCl_2$. The HBSS buffer was replaced and the cells were imaged. An Omega Q-Max Blue filter set (excitation 355−405 nm; emission 420−480 nm) was used. Scale bar: 10 μm.

Summary

Compound **1** undergoes a two-step binding process with Zn^{2+} as shown by ITC and ^{1}H NMR titration studies. The formation of a 2:1 (ligand to Zn^{2+}) complex enables a moderate fluorescence enhancement because of the termination of the photoinduced electron transfer non-radiative process existing in the free ligand. In the presence of Zn^{2+} at higher concentrations, the 1:1 Zn^{2+} complex forms which emits at a longer wavelength with a more pronounced enhancement. Such coordination-mediated photophysical processes of **1** were supported by steady-state spectroscopic studies and fluorescence lifetime measurements, in conjunction with cyclic voltammetry studies and comparison with the properties of other structurally analogous compounds. The revelation of the photophysical variability of compound **1** may shed light on the complex photophysical behaviors of other asymmetrically substituted tripodal type metal coordination ligands.

The potential of **1** in live-cell fluorescence imaging applications was evaluated. Compound **1** is not overly toxic to HeLa cells during the course of our imaging experiment. It penetrates the cell membrane readily and is subsequently retained intracellularly. A clear fluorescence enhancement was observed when cells loaded with **1** were imaged under Zn^{2+}-rich conditions comparing to those imaged under Zn^{2+}-deprived conditions. Further studies are underway to alter the structure of **1** for optimizing the performance of this ligand platform in live-cell imaging studies.

Acknowledgment. This work was supported by Florida State University (FSU) through a start-up fund, a New Investigator Research (NIR) grant from the James and Esther King Biomedical Research Program administered by the Florida Department of Health, and National Science Foundation (CHE 0809201). The efforts by Professor Jack Saltiel and Dr. Bert van de Burgt in securing funds for and setting up the TCSPC accessory are acknowledged. The authors also thank the Institute of Molecular Biophysics at FSU for providing access to a VP-ITC microcalorimeter (Microcal) and Dr. Claudius Mundoma for technical assistance. Dr. Lu Zhang (Argonne National Laboratory) is acknowledged for his initial guidance in ITC studies.

Supporting Information Available: Synthetic procedures and characterization of new compounds, additional spectra, ITC data, and cyclic voltammograms. This material is available free of charge via the Internet at http://pubs.acs.org.